

## Self-Assembly of a Double Calix[6]arene Pseudorotaxane in Oriented Channels

Arturo Arduini,<sup>\*,[a]</sup> Alberto Credi,<sup>\*,[b]</sup> Giovanni Faimani,<sup>[a]</sup> Chiara Massera,<sup>[c]</sup>  
Andrea Pochini,<sup>[a]</sup> Andrea Secchi,<sup>[a]</sup> Monica Semeraro,<sup>[b]</sup> Serena Silvi,<sup>[b]</sup> and  
Franco Ugozzoli<sup>\*,[c]</sup>

**Abstract:** A synthetic study to disclose the more appropriate manner by which two calix[6]arene units could be connected for the construction of an extended tubular structure was undertaken. As a result, a head-to-tail double calix[6]arene having the structure of an oriented nanotube that is about 2.6 nm long and 1.6 nm wide was prepared and characterized. This molecule is able to act as a wheel-type host and forms a supramolecular complex with an axle-type molecule, derived from 4,4'-bipyridinium (viologen), through very efficient self-assembly in solution. The properties of such a pseudorotax-

ane-type complex, which is stabilized by a combination of noncovalent interactions, were investigated in solution by UV/Vis absorption spectroscopy and voltammetric methods. These observations provide a clue about the location of the bipyridinium unit along the nanotube. In the solid state, the complex undergoes a further stage of self-assembly, thereby initiating extend-

ed oriented tubular structures. Crystallographic studies revealed that the positioning of the viologen dication in this asymmetric wheel is addressed by a complicated pattern of cooperative noncovalent intermolecular interactions that involve only one half of the host, whereas the remaining (more polar) half of the host is exploited to create long-range structural order that leads to a "secondary" structure of extended supramolecular channels that, in turn, self-assemble in the lattice, thus giving rise to a "tertiary" structure of parallel sandwiches of nanotubes.

**Keywords:** calixarenes • electrochemistry • ion channels • nanotubes • self-assembly • X-ray diffraction

### Introduction

The construction of systems able to generate channel-like structures is a topic of intense research activity in several scientific fields, such as material sciences, biochemistry, and chemistry. Several strategies for their preparation exist; as an arbitrary selection of examples, molecules that because of the presence of suitable groups appended to a rigid elongated skeleton are able to rearrange and initiate channels or pores have been widely explored.<sup>[1]</sup> Alternatively, a channel-like structure can be achieved through the self-assembly of macrocyclic platforms.<sup>[2]</sup> Within this latter methodology, the calix[4]arene platform has demonstrated its potential to build up these systems.<sup>[3]</sup> In spite of its larger annulus, which could host and possibly allow the passage (transit) of larger species, the calix[6]arene platform has never been employed within this aim.

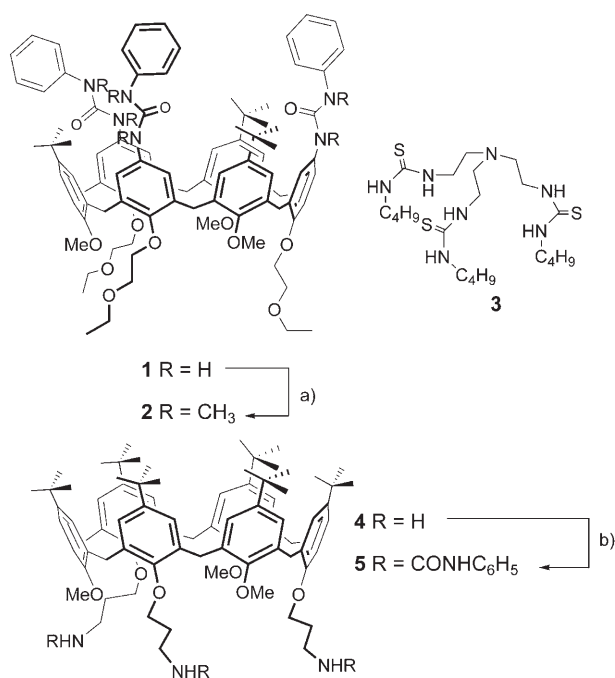
We have, however, recently shown that the triphenylureidocalix[6]arene **1** (Scheme 1) can act as a three-dimensional heteroditopic receptor that can be threaded selectively from the upper rim by suitable axles derived from the 4,4'-bipyri-

[a] Prof. A. Arduini, Dr. G. Faimani, Prof. A. Pochini, Dr. A. Secchi  
Dipartimento di Chimica Organica e Industriale  
Università di Parma  
via G.P. Usberti 17/a, 43100 Parma (Italy)  
Fax: (+39)0521905472  
E-mail: arturo.arduini@unipr.it

[b] Prof. A. Credi, M. Semeraro, Dr. S. Silvi  
Dipartimento di Chimica "G. Ciamician"  
Università di Bologna  
via Selmi 2, 40126, Bologna (Italy)  
Fax: (+39)0512099456  
E-mail: alberto.credi@unibo.it

[c] Dr. C. Massera, Prof. F. Ugozzoli  
Dipartimento di Chimica Generale e Inorganica  
Chimica Analitica, Chimica Fisica  
Università di Parma  
via G.P. Usberti 17/a, 43100 Parma (Italy)  
Fax: (+39)0521905557  
E-mail: franco.ugozzoli@unipr.it

Supporting information for this article is available on the WWW under <http://www.chemistry.org> or from the author.



Scheme 1. Reactions and conditions for the synthesis of calix[6]arene derivatives **2** and **5**: a) NaH, CH<sub>3</sub>I, THF, 70°C, 4 h (83%); b) PhNCO, CH<sub>2</sub>Cl<sub>2</sub>, 3 h (75%). Graphical representation of the receptor **3** for the chloride ion.

dinium (viologen) unit to yield oriented pseudorotaxanes.<sup>[4]</sup> These supramolecular assemblies are endowed with a high thermodynamic stability that derives from the inclusion of the cationic portion of the guest inside the electron-rich cavity and by the interaction of the two counteranions with the three urea moieties.<sup>[5]</sup> The type of counteranions of the bipyridinium-based threads indeed play an important role in the formation of the complex, as they affect both the thermodynamic stability of the complex and the rate of the threading process. These pseudorotaxanes can be reversibly decomposed through electrochemical stimuli.<sup>[6]</sup> This behavior suggests that the calix[6]arene skeleton could be used to build up an extended tubular structure with a wheel as a wall, characterized by a functioning mode that could be traced back to that of molecular machines<sup>[7]</sup> based on pseudorotaxanes.

From analysis of the solid-state structure of the pseudorotaxane formed by **1** and an asymmetrical axle, it emerges that the triphenylureidocalix[6]arene wheel possesses a trigonal prism structure 1.65 nm in length with an internal width of about 0.75 nm (estimated from interatomic distances).<sup>[5]</sup> We, therefore, envisaged that the ability of wheel **1** to yield oriented pseudorotaxanes could be exploited for the construction of oriented asymmetric channel-like structures. However, if the calix[6]arene skeleton should be used to build up a tubular structure, then its inner surface should be extended to approach the length of a bilayer while maintaining all the properties of an asymmetric heteroditopic wheel. To this aim, we envisaged that the linkage of two calix[6]arene units with different hosting properties toward a viologen

guest, connected through an appropriate sequence of binding sites, could meet this criterion. Herein, we report the design, synthesis, and properties of an asymmetric covalently linked double calix[6]arene composed of two calix[6]arene units characterized by the very different binding properties of their inner surfaces.

## Results and Discussion

### Design, synthesis, and characterization of the tubular host:

To establish the most suitable connectivity and relative position of the binding sites within a calixarene dimer, we preliminarily verified whether the three ureido NH groups that are present in **1** are essential in the threading process of the calix[6]arene platform by viologen salts. Therefore, wheel **1** was fully methylated at the NH groups with CH<sub>3</sub>I in the presence of an excess of NaH in THF to give **2** in 83% yield to block the hydrogen-bond donor groups and thus prevent its ability to act as a heteroditopic receptor toward ion pairs (see Scheme 1).

The main features of the <sup>1</sup>H NMR spectrum of **2** (recorded in solution with CDCl<sub>3</sub>) are the signals of the two different *N*-methyl groups at  $\delta=3.04$  and 2.70 ppm, the latter being overlapped with the signals of the three methoxy groups. The signals of all the other protons are broad, and the axial and equatorial methylene protons give rise to two very broad bands at about  $\delta=4.2$  and 3.2 ppm, respectively, thus suggesting a more flexible conformation of **2** with respect to **1**. The ability of **2** to act as a receptor for cations was tested in solution toward dimethyl- (MV<sup>2+</sup>) and dioctylviologen (DOV<sup>2+</sup>) tosylates and monitored through <sup>1</sup>H NMR spectroscopic analysis in CDCl<sub>3</sub>, C<sub>6</sub>D<sub>6</sub>, and CD<sub>3</sub>CN. We found that **2**, probably because of insufficient preorganization and the lack of three binding sites for the recognition of the two anions, could not take up the dialkylviologen salts and form supramolecular complexes in an observable amount. These data suggest that under these conditions the energy gain for complex formation between the cationic portion of the salts employed and the calix[6]arene cavity is not sufficient to overcome the energy needed to separate the cation from the two counteranions in the ion pair. Quite surprisingly, negative evidence of binding was also obtained by adding an excess of **3**, which is an efficient host for the chloride ion,<sup>[8]</sup> to a suspension of **2** and MV<sup>2+</sup> or DOV<sup>2+</sup> as their chloride salts in CDCl<sub>3</sub> (see Scheme 1), thus indicating that the cation and anion binding with distinct hosts (dual-host strategy)<sup>[9]</sup> is less efficient than that afforded by a heteroditopic receptor.<sup>[10]</sup> Indeed the lack of preorganization of **2** in solution was indirectly evidenced from its structure in the solid state (see the Supporting Information for a detailed structure description).

To verify whether the three phenylureido binding sites that are positioned at the upper rim of **1** maintain their function also when they are anchored at the lower rim of the calixarene, derivative **5**, which could in principle still behave as an heteroditopic receptor because of the presence

of the calixarene cavity and the three hydrogen-bond donor groups, was thus synthesized by treating the known 5,11,17,23,29,35-hexa-*tert*-butyl-37,39,41-trimethoxy-38,40,42-tris(3-aminopropoxy)calix[6]arene (**4**)<sup>[11]</sup> with phenylisocyanate (see Scheme 1). Host **5** was submitted to complex formation with MV<sup>2+</sup> or DOV<sup>2+</sup> ditosylate under the same experimental conditions adopted for **2**. These attempts gave, however, negative results as evidenced through NMR spectroscopic and ESI-mass-spectrometric analysis.

The lack of binding ability experienced by **5** and **2** toward the same guests clearly demonstrates that not only are the three urea binding sites essential for binding, but also that they should be positioned in proximity to the calixarene cavity. Thus, a double calix[6]arene should be assembled to maintain the main structural and chemical information present on the reference wheel **1**. We, therefore, considered the possibility of employing three urea moieties for the connection of two calix[6]arene units. From a synthetic point of view, three possible methods exist by which two calixarenes could be covalently connected (Figure 1).

On the basis of the aforementioned considerations, the lower-rim/lower-rim linkage (Figure 1 a) appears as the least promising, since it bears the three ureido bridges positioned at the lower rim of both calixarene subunits. On the other hand, as also previously observed by us,<sup>[12]</sup> the upper-rim/upper-rim linkage (Figure 1 b) yields dimers that show quite poor binding ability toward organic cations. The head-to-tail connecting mode (Figure 1 c) was then chosen for the synthesis of a double calix[6]arene.

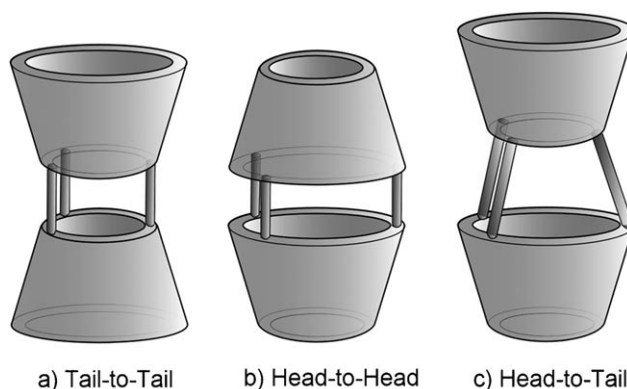
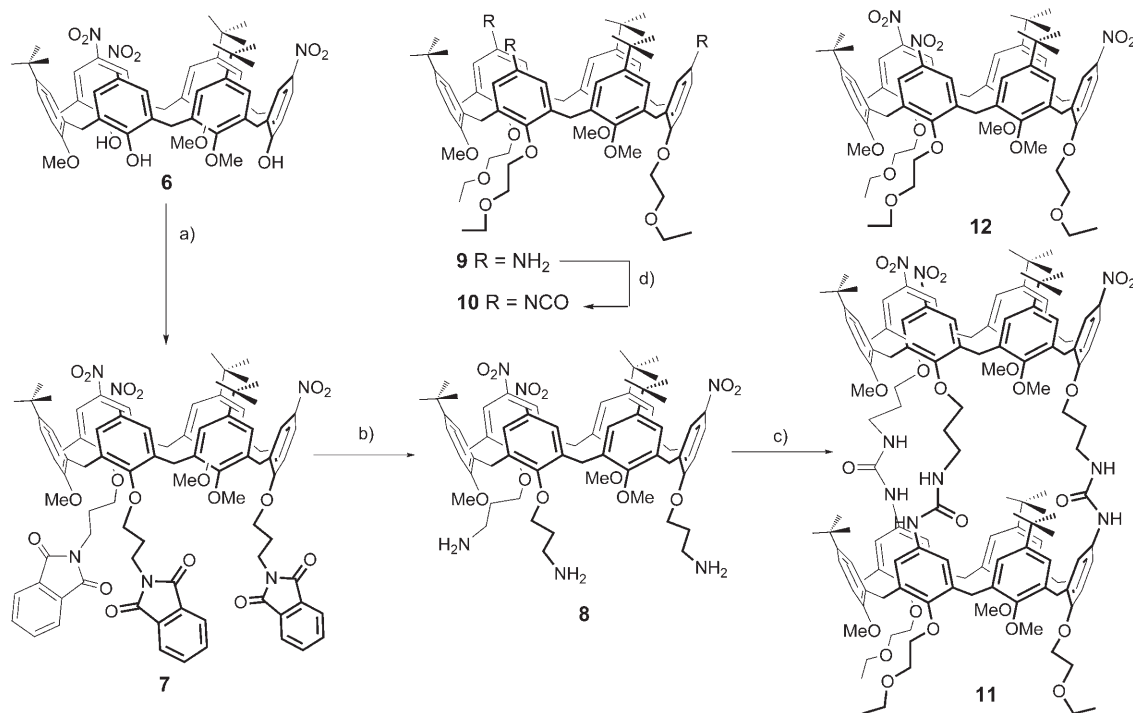


Figure 1. Schematic representation of the three different bridging modes between two calix[6]arenes that afford a tubular structure.

To assign the different binding abilities of the viologen salts toward the two calix[6]arene units of the dimer, it was decided to focus on the hydrogen-bond-acceptor ability of one of the two calixarene units. Therefore, the double calix[6]arene **11** was synthesized in 40% yield starting from the triaminocalix[6]arene derivative **8** and the triisocyanate **10** (see Scheme 2). In **11**, a calix[6]arene unit that bears three ureido moieties at its upper rim is connected through a propyl spacer to the lower rim of a second calixarene unit that bears three electron-withdrawing nitro groups at its upper rim. The <sup>1</sup>H NMR spectra of **11** recorded in several deuterated solvents at room temperature is broad; neverthe-



Scheme 2. Reactions and conditions for the synthesis of the double calix[6]arene **11**: a) K<sub>2</sub>CO<sub>3</sub>, 3-(*N*-bromopropyl)phthalimide, CH<sub>3</sub>CN, reflux, 15 days (30%); b) NH<sub>2</sub>NH<sub>2</sub>·H<sub>2</sub>O, EtOH, reflux, 12 h (90%); c) **10**, CH<sub>2</sub>Cl<sub>2</sub>, 3 h (30%); d) triphosgene, toluene, reflux, 3 h (70%).

less, in  $C_6D_6$  at 330 K (see the Supporting Information) it is sufficiently sharp to allow the complete assignment of all the signals. Under these conditions, the spectrum clearly shows the presence of two sets of signals for the two different calixarene subunits, which both assume a cone conformation on the NMR timescale. In particular, the two doublets at  $\delta=4.47$  and 4.62 ppm were assigned to the pseudoaxial methylene protons of the lower and upper subunits, respectively. The methoxy groups of both subunits resonate as broad singlets at  $\delta=3.1$  and 3.4 ppm, respectively, thus indicating that the methoxy groups of both subunits are oriented inwards toward their corresponding calixarene cavities. As expected, because of the different substitutions of the aromatic ring in the two calixarenes, the aromatic protons of the nitro-substituted unit resonate at  $\delta=8.20$  ppm, whereas those adjacent to the ureido groups resonate at  $\delta=6.94$  ppm. The six chemically different NH protons resonate as two distinct broad signals at  $\delta=5.7$  and 6.9 ppm. The complete assignment of all the signals present in the spectrum of **11** was achieved through 2D NMR DQF-COSY and ROESY techniques (see the Supporting Information).

The addition of the colorless  $DOV(TsO)_2$  (Ts=tosylate) to a solution of **11** in apolar media ( $CDCl_3$  or  $C_6D_6$ ) yielded orange-red solutions from which it was not possible to establish the structure of the species that had formed by using NMR spectroscopic techniques because of the extensive overlapping and broadening of several signals.

**UV/Vis absorption experiments:** We recorded the absorption spectra of  $DOV(TsO)_2$ , double calix[6]arene **11**, and calix[6]arenes **1** and **12** in  $CH_2Cl_2$  at room temperature. The latter two macrocycles can be taken as models for the electron-rich (lower half) and electron-poor (upper half) portions of the double calixarene **11**, respectively (see Scheme 2). All these compounds show intense absorption bands in the near-UV region (see the Supporting Information) and no luminescence.

The absorption spectrum of a 1:1 mixture of calixarene **1** and  $DOV(TsO)_2$  differs from the sum of the spectra of the separated species. Besides the changes in the UV absorption bands of the molecular components, a new broad, weak absorption band of  $\lambda_{max}=465$  nm shows up in the absorption spectrum of the mixture (Figure 2). Spectrophotometric titrations point to the formation of a 1:1 complex with a stability constant of  $(2.0\pm 0.5)\times 10^6$   $M^{-1}$ . The absorption band typical of the supramolecular complex is attributed to charge-transfer (CT) interactions between the electron-rich diphenylureido units of **1** and the viologen unit of  $DOV^{2+}$ , as shown by control experiments carried out on mixtures of  $DOV^{2+}$  and *N,N*-diphenylurea. In fact, we previously showed<sup>[5]</sup> that **1**, and a very similar triphenylureidocalix[6]arene,<sup>[13]</sup> forms a 1:1 pseudorotaxane-type complex with  $DOV^{2+}$  in apolar solvents stabilized by 1) CT interactions between the aromatic rings of the host and bipyridinium guest, 2) hydrogen bonding between the counteranions of the viologen dication and ureidic groups of the wheel, and possibly 3) solvophobic effects on account of the very low solubility of viologen salts in apolar solvents.

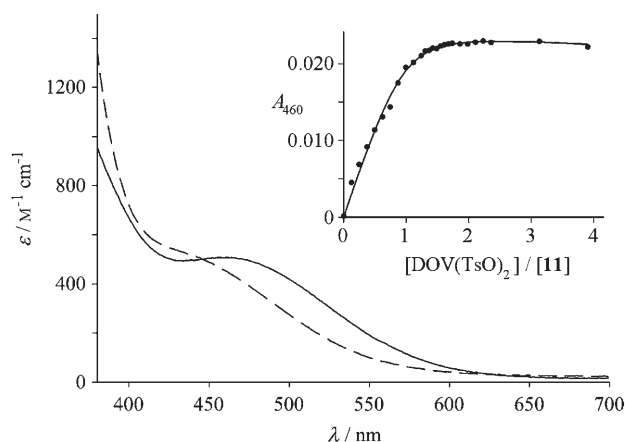


Figure 2. Visible absorption spectra of a solution of the complexes  $[1DOV](TsO)_2$  (full line) and  $[11DOV](TsO)_2$  (dashed line) in  $CH_2Cl_2$ . The inset shows the absorption changes recorded at 460 nm upon addition of  $DOV(TsO)_2$  to a  $1.2\times 10^{-5}$  M solution of **11** in a cell with an optical path length of 5 cm. The curve shows the fitting of the experimental data according to the formation of a 1:1 complex.

Similar behavior was observed in the case of a 1:1 mixture of double calixarene **11** and  $DOV(TsO)_2$ , whose absorption spectrum exhibits a new tail centered at around 440 nm (Figure 2). Spectrophotometric titrations (Figure 2, inset) indicate that a 1:1 complex is formed with a stability constant of  $(1.1\pm 0.3)\times 10^6$   $M^{-1}$ .

As expected, no absorption changes were observed for a 1:1 mixture of host **12** and  $DOV(TsO)_2$  in comparison with the sum of the spectra of the isolated components. The lack of complexation of **12** towards  $DOV^{2+}$  may be related to the fact that the former does not possess an electron-donating cavity (in fact **12** is an electron acceptor). Moreover, **12** is more flexible relative to **1** or **11** and hence poorly preorganized as a host, as evidenced by its  $^1H$  NMR ( $CDCl_3$ ) spectra, in which, for example, the twelve bridging methylene protons resonate as a singlet at  $\delta=4.0$  ppm.

The above results are consistent with the inclusion of the  $DOV^{2+}$  axle into the cavity of nanotube **11**. The similarity between the stability constants of the  $[1DOV](TsO)_2$  and  $[11DOV](TsO)_2$  complexes indicates that the extension of the host inner surface in **11** has not changed the binding efficiency toward viologen salts and, taken together with the lack of complexation of  $DOV^{2+}$  by **12**, suggests that the viologen portion of the axle is surrounded by the electron-rich calix[6]arene unit of **11** (the lower half in Scheme 2). All these observations are in full agreement with the structure observed for the  $[11DOV](TsO)_2$  complex in the solid state (see below). It should be noted that the CT band of the  $[11DOV](TsO)_2$  pseudorotaxane is displaced to higher energy relative to that of the  $[1DOV](TsO)_2$  species (Figure 2), presumably because in the double calixarene **11** the three *N,N*-diphenylureido moieties present in **1** are replaced by less electron-donating phenylureido units.

We also measured the rate constant for the threading of  $DOV(TsO)_2$  into **11** by stopped-flow absorption spectroscopy. The absorption changes recorded over time (see the Sup-



porting Information) could be fitted according to a bimolecular reaction model, thus yielding a second-order rate constant of  $(1.4 \pm 0.1) \times 10^3 \text{ M}^{-1} \text{ s}^{-1}$  at 293 K. This process is much slower than that corresponding to the threading of  $\text{DOV}(\text{TsO})_2$  into a triphenylureidocalix[6]arene very similar to **1** under the same conditions, for which the rate constant was found to be  $(1.7 \pm 0.3) \times 10^6 \text{ M}^{-1} \text{ s}^{-1}$ .<sup>[6]</sup> Previous NMR spectroscopic studies indicate that the insertion of the viologen axle occurs from the upper rim of **1** in apolar solvents.<sup>[4a]</sup> We also pointed out<sup>[6]</sup> that the dissociation of the tight ion pairs between the cationic axle and counteranions and the complexation of the latter by the ureidic units of the host play a major role in determining the self-assembly rate. By hypothesizing a similar process between  $\text{DOV}(\text{TsO})_2$  and **11**, it could be reasonable to assume that the slower self-assembly observed for  $[\mathbf{11} \supset \text{DOV}](\text{TsO})_2$  derives from the fact that the ureidic anion receptors are not located nearby the entrance of the cavity in the double calixarene and thus cannot efficiently assist the dissociation of the  $\text{DOV}(\text{TsO})_2$  ion pairs. The displacement of the viologen axle inside the tubular host, that is, from the upper to lower calixarene moieties, could not be observed in our experiments, most likely because the displacement is too fast on the stopped-flow timescale. Further speculations would be unsafe because we did not investigate the self-assembly kinetics in sufficient detail (e.g., the energy barrier was not determined).

**Voltammetric experiments:** Electrochemical techniques are particularly useful for investigating the behavior of the axle unit inside the calixarene wheels as a result of the valuable redox properties of the viologen salts.<sup>[14]</sup> It should be noted that since the electrochemical experiments are carried out in the presence of a large excess of tetrabutylammonium hexafluorophosphate, used as a supporting electrolyte, the cationic species are present in solution as ion pairs with the  $\text{PF}_6^-$  ions.  $\text{DOV}(\text{PF}_6)_2$  shows<sup>[15]</sup> the two typical reversible monoelectronic processes ( $E_{1/2} = -0.28$  and  $-0.82$  V versus the saturated calomel electrode (SCE); Figure 3) and no ox-

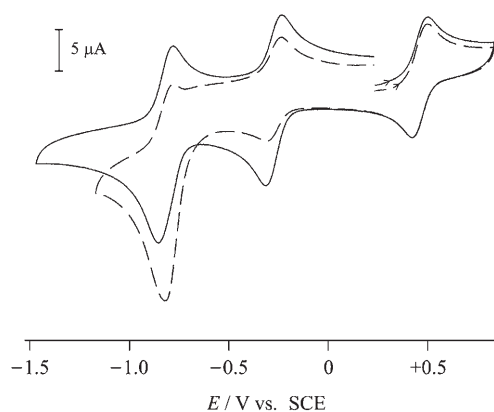


Figure 3. Cyclic voltammetric curves for the reduction of  $\text{DOV}^{2+}$  alone (full line) and in the presence of one equivalent of the double calixarene **11** (dashed line). Conditions:  $\text{CH}_2\text{Cl}_2$ ,  $2.2 \times 10^{-4}$  M, 0.02 M tetrabutylammonium hexafluorophosphate,  $0.3 \text{ V s}^{-1}$ , glassy carbon electrode. The reversible wave at  $+0.46$  V versus SCE is ferrocene used as an internal reference.

idation processes. Calixarenes **1** and **12** and double calixarene **11** exhibit several irreversible oxidation processes at potentials higher than  $E = +1.0$  V, assigned to the oxidation of their electron-rich aromatic units.<sup>[16]</sup> Calixarene **1** shows no reduction processes in the potential window examined, whereas **11** and **12** exhibit irreversible processes at  $E < -1.2$  V, which we assigned to the reduction of their nitro-substituted aromatic units.<sup>[16]</sup> For the sake of the discussion and because of the irreversibility of the redox processes of the hosts, we will consider only the reduction processes of the viologen unit in the various compounds.

The electrochemical behavior of the  $[\mathbf{1} \supset \text{DOV}](\text{PF}_6)_2$  pseudorotaxane on reduction (see the Supporting Information) is nearly identical to that previously observed<sup>[6]</sup> for a very similar system. The cyclic voltammetric wave for the first reduction of the viologen unit in the complex is characterized by a large separation between the cathodic and anodic peaks. The cathodic wave ( $E_p = -0.63$  V at a scan rate of  $0.3 \text{ V s}^{-1}$ ) is negatively shifted by more than 330 mV with respect to that of  $\text{DOV}(\text{PF}_6)_2$  alone, whereas the corresponding anodic wave ( $E_p = -0.23$  V) occurs at nearly the same potential as that of free  $\text{DOV}(\text{PF}_6)_2$ . The second reduction process is reversible and takes place at a potential ( $E_{1/2} = -0.82$  V) identical to that of the free axle, thus indicating that a one-electron reduction of the viologen unit causes the dethreading from the host. The behavior observed for the first reduction process of  $[\mathbf{1} \supset \text{DOV}](\text{PF}_6)_2$  can be accounted for by the fact that 1) the viologen dication is stabilized by inclusion into the calixarene wheel and 2) the (re)threading of the electrochemically regenerated  $\text{DOV}^{2+}$  axle into **1** is slow on the timescale of the voltammetric experiment.<sup>[6]</sup>

The  $[\mathbf{11} \supset \text{DOV}](\text{PF}_6)_2$  pseudorotaxane exhibits, as expected, the two monoelectronic reductions of its viologen axle ( $E_{1/2} = -0.27$  and  $-0.82$  V; Figure 3). The fact that the viologen unit is associated with the double calixarene host<sup>[17]</sup> is reflected by the decrease in the current intensity of the voltammetric waves, because of the smaller diffusion coefficient of the complex. In contrast with the behavior of the monocalixarene pseudorotaxane described above, the first reduction process is reversible and occurs at a potential value almost equal to that of the same process in the free axle. The second reduction wave is affected by adsorption phenomena; its potential appears to be not shifted relative to the same wave in the free  $\text{DOV}^{2+}$  axle. The lack of a potential shift in the first reduction wave (Figure 3) is a somewhat surprising result because the absorption data indicate that the viologen unit is involved in CT interactions with the host. Moreover, while we found that encapsulation of the viologen unit into a triphenylureidocalix[6]arene wheel causes a decrease in the heterogeneous electron-transfer rate constant,<sup>[6]</sup> the first reduction wave of  $\text{DOV}^{2+}$  complexed by **11** is electrochemically reversible under our conditions, thus indicating a relatively fast heterogeneous electron-transfer process.

These observations can be accounted for by the fact that the viologen unit may exhibit some mobility along the tubu-

lar host, thereby spending some of its time close to the region of connection of the two calixarene halves. Inspection of molecular models (see also Figure 4) shows that in such a position the viologen unit 1) is no longer surrounded by

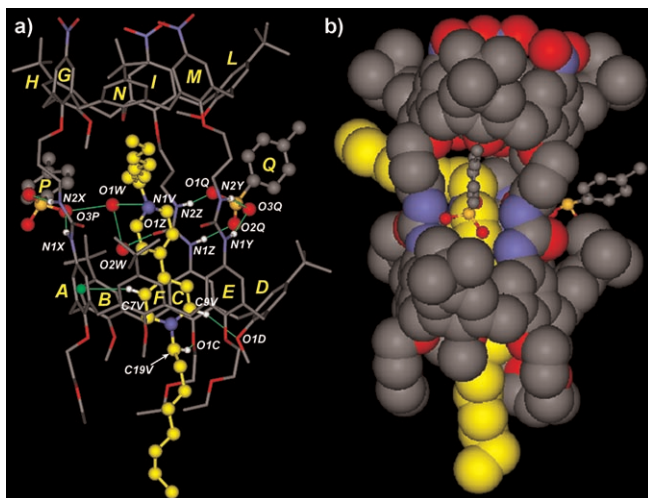


Figure 4. X-ray structure of the complex  $[11]DOV(TsO)_2$  (the  $DOV^{2+}$  component is yellow). a) Partial stick view; b) partial space-filling view. Only the hydrogen atoms involved in weak, attractive intermolecular interactions are shown. The hydrogen bonds and CH- $\pi$  interactions are denoted by green lines.

electron-rich aromatic moieties, 2) is not effectively encapsulated because of the presence of relatively large portals between the spacers that link the two calixarene halves,<sup>[18]</sup> and 3) may come in contact with external molecules (solvent or anions). Therefore, it can be expected that in such a supramolecular conformation the electrochemical properties of the viologen unit may not be affected too much by the host (apart from the decrease in current intensity as a result of the smaller diffusion coefficient). The fate of the complex between **11** and the viologen axle upon reduction of the latter is difficult to assess on the basis of the redox potential values.

**X-ray structure of the supramolecular complex:** Crystals suitable for X-ray analysis were obtained from the slow evaporation of the reddish solution obtained by mixing **11** and  $DOV(TsO)_2$  in benzene/methanol.

In the solid state, four chemical species, namely, the neutral host **11**,  $DOV^{2+}$ , the two tosylate anions, and two water molecules, self-assemble in a supramolecular complex (see Figure 4) that belongs to the pseudorotaxane class and has the shape of a trigonal prism of about  $2.6 \times 1.6$  nm. In the complex, the two aromatic domains are characterized by different hydrogen-bond-acceptor abilities and are also slightly different in size and shape (see the Supporting Information for an unequivocal description of the calix[6]arene conformations).

The dicationic thread is positioned within the ABCDEF cavity through a system of weak intermolecular attractive interactions, and one of its octyl chains protrudes from the lower rim of this latter subunit. The other octyl chain ex-

tends outside the dimer through the portals of the equatorial plane of **11**, probably because the cavity of the second calix[6]arene unit GHILMN is partially obstructed by the methoxy groups of rings L and N and by the highly polar character of the inner surface of this latter macrocycle. Two adventitious water molecules are also present in the host, while, as expected, the two tosylate anions are confined outside **11** in proximity to the three urea moieties. All components are held together by the simultaneous cooperation of strong, non-directional electrostatic interactions between the charged species and weak, highly directional (and thus selective) intermolecular interactions, such as hydrogen bonds and CH- $\pi$  interactions. The geometrical parameters for the weak attractive interactions in the complex are listed in the Supporting Information.

A set of multiple weak attractions between the calixarene ABCDEF and viologen units are responsible of the asymmetric position of the guest within the cavity. The strongest attraction is the hydrogen bond  $C9V-H \cdots O1D$  ( $O1D \cdots H = 2.207(9)$ ;  $C9V \cdots O1D = 3.156(9)$  Å). Contemporarily, the hydrogen atom on C7V points toward the centroid of the phenolic ring A, thus giving rise to a CH- $\pi$  interaction with the hydrogen atom at  $2.658(9)$  Å over the centroid of phenolic ring A. This value is significantly shorter than the value of  $2.84$  Å calculated by Tsuzuki et al. in the high-level ab initio calculation of the benzene/methane interaction in the gas phase,<sup>[19]</sup> when the methane C-H bond is orthogonal to the benzene centroid. A third (weaker) hydrogen bond  $C19V-H \cdots O1C$  ( $O1C \cdots H = 2.489(9)$ ;  $C19V \cdots O1C = 3.310(9)$  Å) involves one hydrogen atom at the terminal aliphatic chain of the guest and the phenolic oxygen atom of ring C. These interactions are superimposed onto the electrostatic attractions that occur between the doubly charged guest and the two tosylate anions. These latter species are also involved in multiple weak attractive interactions involving simultaneously the host and the two water molecules inside the host cavity and play different roles. In particular, anion Q forms four hydrogen bonds with the urea chains of the host: two of them through O3Q, which acts as acceptor of the two hydrogen bonds  $O3Q \cdots H-N1Y$  ( $O3Q \cdots H = 2.058(9)$ ;  $O3Q \cdots N1Y = 2.968(9)$  Å) and  $O3Q \cdots H-N2Y$  ( $O3Q \cdots H = 2.032(9)$ ;  $O3Q \cdots N2Y = 2.942(9)$  Å); the other two oxygen atoms O1Q and O2Q act as acceptors of the two hydrogen bonds  $O1Q \cdots H-N2Z$  ( $O1Q \cdots H = 1.993(9)$ ;  $O1Q \cdots N2Z = 2.937(9)$  Å) and  $O2Q \cdots H-N1Z$  ( $O2Q \cdots H = 1.928(9)$ ;  $O2Q \cdots N1Z = 2.846(9)$  Å). In any case the role of the urea NH groups is crucial for the binding of the two tosylate anions through hydrogen bonding. The tosylate Q simultaneously interacts with the urea groups of chains Y and Z (Figure 4a), whereas the anion P interacts with the NH groups of chain X.

The role of the second anion P is quite different and more important in stabilizing the supramolecular architecture of the complex. In fact, the oxygen atom O2P links the host through the single hydrogen bond  $O2P \cdots H-N2X$  ( $O2P \cdots H = 1.978(9)$ ;  $O2P \cdots N2X = 2.927(9)$  Å). At the same time, the oxygen atom O3P connects with the anion P, the two water

molecules within the cavity, and the guest dication. In fact, this oxygen atom accepts one hydrogen bond from the host,  $O3P \cdots H-N1X$  ( $O3P \cdots H = 1.961(9)$ ;  $O3P \cdots N1X = 2.879(9)$  Å), and contemporarily shows a hydrogen-bond contact with oxygen atom O1W of one of the two water molecules, which in turn is linked to the host and dication through two hydrogen-bond contacts: one with N1V of the dication ( $O1W \cdots N1V = 3.170(9)$  Å) and a second with the second water molecule O2W within the host cavity ( $O1W \cdots O2W = 2.68(1)$  Å). The stability of the complex is further enhanced by another hydrogen-bond contact between O2W and O1Z with a donor-acceptor distance of 2.952(8) Å. Through this way, the role of the two water molecules within the host cavity is only limited, thus enhancing the stability of the complex and appearing unable to influence the position of the dioctylviologen within the host cavity.

In the crystal, the asymmetry of the complex is responsible for the formation of a “secondary” structure that results in the formation of an oriented “channel-like” structure. In fact, the aliphatic chain that protrudes from the calixarene ABCDEF of one complex acts as a dominant structure-directing factor by entering into the calixarene GHILMN of another complex, thus filling the space in the NO<sub>2</sub> region (Figure 5a). The “pitch” along a single channel is 22.424 Å, and each adjacent parallel channel is shifted in that direction by one half of the pitch (11.212 Å).

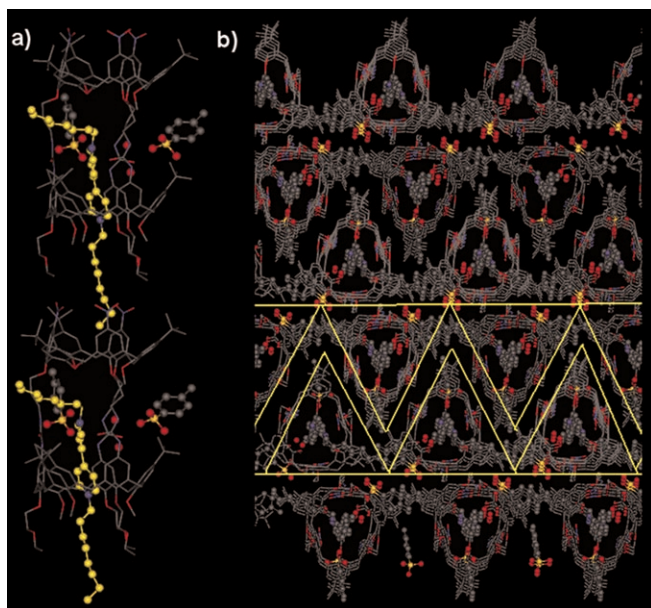


Figure 5. a) Self-assembly in a columnar arrangement of the supramolecular complexes in the nanotube “secondary” structure. Hydrogen atoms have been omitted for clarity. b) Self-assembly of the nanotubes in the crystal lattice give rise to a “tertiary” structure of sandwiched bilayers of nanotubes (a bilayer is evidenced between the two horizontal yellow lines).

A third structural motif (a “tertiary” structure) is observed in the self-assembly of the channels (Figure 5b) in

the plane orthogonal to the axis of the tubules, thus giving rise to a sandwich superstructure of segregated bilayers (of about 19.5 Å in thickness, calculated as interatomic distances) of nanotubes. Although each bilayer is electrically uncharged, the two surfaces of each bilayer are strongly polar as a result of the presence of the external SO<sub>3</sub><sup>-</sup> groups.

## Conclusions

We have shown that a tubular molecular host containing predetermined chemical functionalities can be obtained by appropriately linking two calix[6]arene units. The length of this calixarene dimer is comparable to the thickness of a bilayer membrane, while its diameter is suitable for the encapsulation of aromatic rings. In fact, we have shown that this compound is able to function as a dissymmetric heteropolytopic host, thus forming a fairly stable pseudorotaxane-type complex with dioctylviologen in apolar solvents. In the solid state, the supramolecular complexes self-assemble to yield a “secondary” arrangement of extended channels, which in turn give rise to a “tertiary” structure of parallel sandwiches of nanotubes.

These results show that our approach is promising for the construction of functional self-assembling structures at the nanoscale. More specifically, pseudorotaxane-type complexes based on extended and dissymmetric (oriented) tubular hosts may constitute a promising platform for the realization of artificial molecular channels that can be controlled by external stimuli. Studies are undergoing in our laboratories to exploit this approach and for the preparation of new working tubular devices.

## Experimental Section

**General:** All the reactions were carried out under nitrogen, and all the solvents were freshly distilled under nitrogen and stored over molecular sieves for at least 3 h prior to use. All the other reagents were of reagent-grade quality as obtained from commercial suppliers and were used without further purification. Column chromatography was performed on silica gel (63–200 mesh). The NMR spectra were recorded in CDCl<sub>3</sub> unless otherwise indicated. Mass spectra were determined in ESI mode. The melting points are uncorrected. The elemental analyses were carried out at the Laboratory of Microanalysis, Dipartimento Farmaceutico, University of Parma. Compounds **1**,<sup>[20]</sup> 5,11,17,23,29,35-hexa-*tert*-butyl-37,39,41-trimethoxy-38,40,42-tris(3-aminopropoxy)calix[6]arene (**4**),<sup>[11]</sup> 5,17,29-tri-*tert*-butyl-11,23,35-trinitro-37,39,41-trimethoxycalix[6]arene (**6**),<sup>[20]</sup> 5,17,29-tri-*tert*-butyl-11,23,35-triamino-37,39,41-trimethoxy-38,40,42-tris(2-ethoxyethoxy)calix[6]arene (**9**),<sup>[20]</sup> and 5,17,29-tri-*tert*-butyl-11,23,35-trinitro-37,39,41-trimethoxy-38,40,42-tris(2-ethoxyethoxy)calix[6]arene (**12**)<sup>[20]</sup> were synthesized according to literature procedures. ***N,N*-Hexamethyltriphenylureidocalix[6]arene (2):** A solution of calix[6]arene **1** (0.23 g, 0.16 mmol) and NaH (60% in oil, 0.075 g, 1.88 mmol) in dry THF (20 mL) was poured in a thick-walled glass autoclave and heated at 70 °C for 30 min. The solution was cooled to room temperature, and CH<sub>3</sub>I (0.26 g, 1.88 mmol) added. The resulting mixture was kept at 70 °C for a further 4 h, cooled to room temperature, diluted with ethyl acetate (50 mL), and quenched with a 10% aqueous solution of HCl (25 mL, CAUTION!). The separated organic phase was washed to neutrality with brine and dried over anhydrous Na<sub>2</sub>SO<sub>4</sub>. The solvent removed

to dryness under reduced pressure. The crude brownish oily residue was purified by column chromatography (hexane/ethyl acetate 1:1, then 4:6) to afford **2** (0.20 g, 83%) as a yellowish solid. M.p. 108–110 °C;  $^1\text{H NMR}$  (300 MHz,  $\text{C}_6\text{D}_6$ ):  $\delta$  = 1.14 (t,  $^3J(\text{H,H})$  = 7 Hz, 9H,  $\text{OCH}_2\text{CH}_3$ ), 1.41 (s, 27H,  $\text{C}(\text{CH}_3)_3$ ), 2.77 (bs, 9H,  $\text{ArOCH}_3$ ), 2.86 (s, 9H,  $\text{Ar}(\text{calix})\text{NCH}_3$ ), 3.14 (s, 9H,  $\text{PhNCH}_3$ ), 3.2 (bs, 6H,  $\text{ArCH}_2\text{Ar}$ , equatorial), 3.43 (q,  $^3J(\text{H,H})$  = 7 Hz, 6H,  $\text{OCH}_2\text{CH}_3$ ), 3.61 (t,  $^3J(\text{H,H})$  = 5 Hz, 6H,  $\text{ArOCH}_2\text{CH}_2\text{O}$ ), 3.82 (t,  $^3J(\text{H,H})$  = 5 Hz, 6H,  $\text{ArOCH}_2\text{CH}_2\text{O}$ ), 4.6 (bs, 6H,  $\text{ArCH}_2\text{Ar}$  axial), 6.3–6.8 and 7.4 ppm (m and bs, 27H,  $\text{Ar}(\text{calix})\text{-H}$  and  $\text{Ph-H}$ );  $^{13}\text{C NMR}$  (75 MHz,  $\text{C}_6\text{D}_6$ )  $\delta$  = 15.6, 30.3, 31.9, 34.4, 38.9, 39.3, 60.7, 66.9, 70.1, 72.9, 124.4, 125.0, 125.9, 126.9, 127.2, 133.6, 135.0, 141.8, 146.0, 146.5, 151.6, 155.1, 160.5 ppm; ESI-MS:  $m/z$  (%): 797.5 (100) [ $M+2\text{Na}^+$ ]/2, 1572.0 (15) [ $M+\text{Na}^+$ ].

**Calix[6]arene (5):** A solution of calix[6]arene **4** (0.48 g, 0.41 mmol) and phenylisocyanate (0.24 g, 2 mmol) in  $\text{CH}_2\text{Cl}_2$  (25 mL) was stirred at room temperature. After 3 h, the solvent was completely evaporated under reduced pressure. Purification of the solid residue by column chromatography (hexane/ethyl acetate 6:5) afforded **5** (0.47 g, 75%) as a white solid. M.p. 205–208 °C;  $^1\text{H NMR}$  (300 MHz,  $\text{CDCl}_3$ ):  $\delta$  = 0.93 (s, 27H,  $\text{C}(\text{CH}_3)_3$ ), 1.25 (s, 27H,  $\text{C}(\text{CH}_3)_3$ ), 1.8 (bs, 6H,  $\text{OCH}_2\text{CH}_2\text{CH}_2\text{NH}$ ), 2.65 (s, 6H,  $\text{OCH}_3$ ), 3.41 (bs, 6H,  $\text{OCH}_2\text{CH}_2\text{CH}_2\text{NH}$ ), 3.46 (d, 6H,  $^2J(\text{H,H})$  = 15 Hz,  $\text{ArCH}_2\text{Ar}$  equatorial), 3.9 (bs, 6H,  $\text{OCH}_2\text{CH}_2$ ), 4.47 (d, 6H,  $^2J(\text{H,H})$  = 15 Hz,  $\text{ArCH}_2\text{Ar}$  axial), 5.7 (bt, 3H,  $\text{CH}_2\text{NH}$ ), 6.80 (s, 6H,  $\text{Ar}(\text{calix})\text{-H}$ ), 6.96 (t, 3H,  $^3J(\text{H,H})$  = 7 Hz,  $\text{Ph-H}_{(\text{para})}$ ), 7.04 (s, 3H,  $\text{PhNH}$ ), 7.13 (s, 6H,  $\text{Ar}(\text{calix})\text{-H}$ ), 7.2–7.3 ppm (m, 12H,  $\text{Ph-H}_{(\text{ortho,meta})}$ );  $^{13}\text{C NMR}$  (75 MHz,  $\text{CDCl}_3$ ):  $\delta$  = 30.1, 30.3, 31.4, 31.7, 34.3, 34.5, 37.2, 60.8, 72.8, 120.5, 124.0, 125.8, 127.5, 129.1, 133.1, 133.5, 139.5, 146.4, 146.7, 152.0, 153.6, 168.5 ppm; ESI-MS:  $m/z$  (%): 1566 (100) [ $M+\text{Na}^+$ ]; elemental analysis calcd (%) for  $\text{C}_{99}\text{H}_{126}\text{N}_6\text{O}_9$  (1544.1): C 77.01, H 8.22, N 5.44; found: C 76.87, H 8.40, N 5.41.

**Calix[6]arene (7):**  $\text{K}_2\text{CO}_3$  (1 g, 7.14 mmol) was added to a solution of calixarene **6** (1 g, 1.02 mmol) and *N*-(3-bromopropyl)phtalimide (2.5 g, 9.2 mmol) in acetonitrile (50 mL). The resulting heterogeneous mixture was heated under reflux for 15 days, and then the solvent was evaporated to dryness under reduced pressure. The solid residue was taken up with  $\text{CH}_2\text{Cl}_2$ , and the resulting organic phase washed with a 10% aqueous solution of HCl and water until neutral. The separated organic layer was dried over  $\text{Na}_2\text{SO}_4$ , and the solvent evaporated to dryness under reduced pressure. Purification of the solid residue by column chromatography (hexane/ethyl acetate 6:4) afforded **7** (0.47 g, 30%) as a yellowish solid. M.p. 257–260 °C;  $^1\text{H NMR}$  (300 MHz,  $\text{CDCl}_3$ ):  $\delta$  = 1.31 (s, 27H,  $\text{C}(\text{CH}_3)_3$ ), 2.25 (bs, 6H,  $\text{OCH}_2\text{CH}_2\text{CH}_2\text{N}$ ), 2.89 (s, 9H,  $\text{ArOCH}_3$ ), 3.5 (bs, 6H,  $\text{ArCH}_2\text{Ar}$  equatorial), 3.9 (bs, 12H,  $\text{OCH}_2\text{CH}_2\text{CH}_2\text{N}$ ), 4.3 (bs, 6H,  $\text{ArCH}_2\text{Ar}$  axial), 7.2 and 7.6 (2bs, 12H,  $\text{Ar}(\text{calix})\text{-H}$ ), 7.6–7.8 ppm (m, 12H,  $\text{Ar-H}_{(\text{phtal})}$ );  $^{13}\text{C NMR}$  (75 MHz,  $\text{CDCl}_3$ ):  $\delta$  = 29.4, 30.9, 31.4, 34.2, 35.2, 59.9, 71.3, 123.2, 127.4, 131.9, 132.0, 133.9, 135.9, 143.8, 146.9, 159.3, 168.2 ppm; ESI-MS:  $m/z$  (%): 1565 (100) [ $M+\text{Na}^+$ ], 1581 (45) [ $M+\text{K}^+$ ].

**Calix[6]arene (8):**  $\text{N}_2\text{H}_4\cdot\text{H}_2\text{O}$  (0.93 g, 18 mmol) was added to a suspension of **7** (0.56 g, 0.36 mmol) in absolute ethanol (50 mL), and the resulting mixture was refluxed overnight. The solvent was then removed under reduced pressure, and the solid residue taken up in  $\text{CH}_2\text{Cl}_2$  (20 mL). The resulting organic solution was washed with water and dried over  $\text{Na}_2\text{SO}_4$ . The solvent was evaporated under reduced pressure to afford **8** (0.37 g, 90%) as a yellow solid. M.p. 162–165 °C;  $^1\text{H NMR}$  (300 MHz,  $\text{CDCl}_3$ ):  $\delta$  = 1.24 (s, 27H,  $\text{C}(\text{CH}_3)_3$ ), 1.7–1.9 (m, 12H,  $\text{OCH}_2\text{CH}_2\text{CH}_2\text{NH}_2$ ), 2.81 (t,  $^3J(\text{H,H})$  = 6 Hz, 6H,  $\text{OCH}_2\text{CH}_2\text{CH}_2\text{NH}_2$ ), 2.96 (s, 9H,  $\text{ArOCH}_3$ ), 3.78 (t,  $^3J(\text{H,H})$  = 6 Hz, 6H,  $\text{OCH}_2\text{CH}_2\text{CH}_2\text{NH}_2$ ), 3.87 (s, 12H,  $\text{ArCH}_2\text{Ar}$ ), 7.11 and 7.73 ppm (2s, 12H,  $\text{Ar}(\text{calix})\text{-H}$ );  $^{13}\text{C NMR}$  (75 MHz,  $\text{CDCl}_3$ ):  $\delta$  = 30.7, 31.3, 33.5, 34.2, 38.8, 60.0, 71.7, 123.5, 127.0, 132.0, 135.9, 143.6, 146.8, 154.0, 160.1 ppm; ESI-MS:  $m/z$  (%): 1153 (60) [ $M+\text{H}^+$ ].

**Calix[6]arene (10):** A solution of calix[6]arene **9** (0.12 g, 0.11 mmol) in dry toluene (50 mL) was dropwise added over a period of 1 h to a solution of bis(trichloromethyl)carbonate (0.04 g, 0.14 mmol) in dry toluene (100 mL). The resulting mixture was refluxed for 3 h, and then the solvent was completely evaporated under reduced pressure. The crude residue was triturated with hot hexane (5 mL), and the solid suspension filtered off. Removal of the solvent filtrate under reduced pressure afforded **10** (0.09 g, 70%) as a white solid. M.p. 75–77 °C;  $^1\text{H NMR}$  (300 MHz,

$\text{CDCl}_3$ ):  $\delta$  = 1.19 (t,  $^3J(\text{H,H})$  = 7 Hz, 9H,  $\text{OCH}_2\text{CH}_3$ ), 1.31 (s, 27H,  $\text{C}(\text{CH}_3)_3$ ), 2.89 (s, 9H,  $\text{ArOCH}_3$ ), 3.55 (q,  $^3J(\text{H,H})$  = 7 Hz, 6H,  $\text{OCH}_2\text{CH}_3$ ), 3.6–4.2 (m, 24H,  $\text{OCH}_2\text{CH}_2\text{O}$ ,  $\text{ArCH}_2\text{Ar}$ ), 6.48 and 7.16 ppm (2s, 12H,  $\text{Ar}(\text{calix})\text{-H}$ );  $^{13}\text{C NMR}$  (75 MHz,  $\text{CDCl}_3$ ):  $\delta$  = 15.2, 30.3, 31.5, 34.2, 60.0, 66.6, 69.6, 72.3, 123.5, 125.5, 127.2, 128.4, 132.7, 136.0, 146.3, 152.1, 154.4 ppm; ESI-MS:  $m/z$  (%): 1028 (20) [ $M+\text{Na}^+$ ].

**Bis(calix[6]arene (11):** A solution of **8** (0.21 mg, 0.18 mmol) in  $\text{CH}_2\text{Cl}_2$  (100 mL) was added to a solution of **10** (0.2 g, 0.18 mmol) in  $\text{CH}_2\text{Cl}_2$  (200 mL) with vigorous stirring. The resulting mixture was stirred at room temperature for a further 3 h, and then the solvent was removed under reduced pressure. Purification of the residue by column chromatography (dichloromethane/ethyl acetate 4:6) afforded **11** (0.13 g, 30%) as a white solid. M.p. 150 °C (decomp);  $^1\text{H NMR}$  (300 MHz,  $\text{C}_6\text{D}_6$ , 330 K):  $\delta$  = 1.09 (s, 27H,  $\text{Ar}(\text{calixdown})\text{-C}(\text{CH}_3)_3$ ), 1.25 (t,  $^3J(\text{H,H})$  = 7 Hz, 9H,  $\text{OCH}_2\text{CH}_3$ ), 1.44 (s, 27H,  $\text{Ar}(\text{calixup})\text{-C}(\text{CH}_3)_3$ ), 1.9 (bs, 6H,  $\text{OCH}_2\text{CH}_2\text{CH}_2\text{N}$ ), 3.09 (s, 9H,  $\text{Ar}(\text{calixup})\text{-OCH}_3$ ), 3.35 (d,  $^2J(\text{H,H})$  = 15 Hz, 6H,  $\text{ArCH}_2\text{Ar}_{(\text{up})}$  equatorial), 3.5 (bs, 15H,  $\text{Ar}(\text{calixdown})\text{-OCH}_3$  and  $\text{OCH}_2\text{CH}_2\text{CH}_2\text{N}$ ), 3.55 (q,  $^4J(\text{H,H})$  = 7 Hz, 6H,  $\text{OCH}_2\text{CH}_3$ ), 3.6 (bs, 6H,  $\text{OCH}_2\text{CH}_2\text{CH}_2\text{N}$ ), 3.7–3.8 (m, 12H,  $\text{OCH}_2\text{CH}_2\text{O}$  and  $\text{ArCH}_2\text{Ar}_{(\text{calixdown})}$  equatorial), 4.0 (bs, 6H,  $\text{OCH}_2\text{CH}_2\text{O}$ ), 4.48 (d,  $^2J(\text{H,H})$  = 15 Hz, 6H,  $\text{ArCH}_2\text{Ar}_{(\text{calixup})}$  axial), 4.69 (d,  $^2J(\text{H,H})$  = 15 Hz, 6H,  $\text{ArCH}_2\text{Ar}_{(\text{calixdown})}$  axial), 6.9 (bs, 6H,  $\text{Ar}(\text{calixdown})\text{-H}$ ), 6.99 (s, 6H,  $\text{Ar}(\text{calixdown})\text{-H}$ ), 7.46 and 8.19 ppm (2s, 12H,  $\text{Ar}(\text{calixup})\text{-H}$ );  $^{13}\text{C NMR}$  (75 MHz,  $\text{CDCl}_3$ ):  $\delta$  = 15.5, 31.2, 31.7, 34.3, 60.4, 61.2, 66.7, 70.1, 72.4, 72.8, 124.8, 125.6, 125.8, 125.9, 129.3, 132.1, 136.1, 144.2, 146.6, 147.2, 151.5, 153.8, 157.4, 160.2 ppm; ESI-MS:  $m/z$  (%): 1193 (100) [ $M+2\text{Na}^+$ ]/2, 2363 (15) [ $M+\text{Na}^+$ ]; elemental analysis calcd (%) for  $\text{C}_{138}\text{H}_{171}\text{N}_6\text{O}_{24}\cdot\text{H}_2\text{O}$  (2357.9): C 70.29, H 7.40, N 5.35; found: C 70.05, H 7.42, N 5.29.

**UV/Vis absorption spectroscopy:** Measurements were carried out at room temperature (ca. 295 K) in air-equilibrated (Merck Uvasol) solutions in  $\text{CH}_2\text{Cl}_2$  in the concentration range  $1 \times 10^{-5}$ – $2 \times 10^{-4}$  M. The UV/Vis absorption spectra were recorded on a Perkin–Elmer  $\lambda$ 40 spectrophotometer. Reaction kinetic profiles were collected for air-equilibrated solutions in  $\text{CH}_2\text{Cl}_2$  at 293 K with an Applied Photophysics SX18MV stopped-flow spectrophotometer interfaced to a PC. Under the conditions employed, the time required to fill the observation cell (1-cm path length) was experimentally determined to be <1.3 ms (based on a test reaction). The concentration of the reactants after mixing was on the order of  $1 \times 10^{-5}$  M. The absorption titration and kinetic curves were analyzed with the SPECFIT software.<sup>[21]</sup> Experimental errors: wavelength values:  $\pm 1$  nm; absorption coefficients:  $\pm 10\%$ . For more details, see ref. [6].

**Voltammetric experiments:** Cyclic voltammetric (CV) and differential-pulse voltammetric (DPV) experiments were carried out in argon-purged  $\text{CH}_2\text{Cl}_2$  (Romil Hi-Dry) with an Autolab 30 multipurpose instrument interfaced to a PC. The working electrode was a glassy carbon electrode (Amel; 0.07  $\text{cm}^2$ ), the counter electrode was a Pt wire (separated from the solution by a frit), and an Ag wire was employed as a quasireference electrode. Ferrocene was present as an internal standard. The concentration of the compounds examined was on the order of  $2 \times 10^{-4}$  M; tetrabutylammonium hexafluorophosphate (0.02 M) was added as a supporting electrolyte. Under these conditions, the observed potential window ranged from –2.0 to +1.6 V versus SCE. Cyclic voltammograms were obtained at sweep rates of 0.02–1  $\text{Vs}^{-1}$ . Differential-pulse voltammograms were obtained at a sweep rate of 0.02  $\text{mVs}^{-1}$ , with a pulse height of 75 mV and a duration of 40 ms. The IR compensation implemented within the Autolab 30 was used, and every effort was made throughout the experiments to minimize the resistance of the solution. In any instance, the full electrochemical reversibility of the voltammetric wave of ferrocene was taken as an indicator of the absence of uncompensated resistance effects. For reversible processes, the half-wave potential values were calculated from an average of the CV and DPV experiments, whereas the redox potential values in the case of irreversible processes were estimated from the DPV peaks. Experimental errors: potential values:  $\pm 10$  mV for reversible processes,  $\pm 20$  mV for irreversible processes. For more details, see ref. [6].

**X-ray crystallographic studies:** Intensity data were collected using  $\text{MoK}\alpha$  radiation ( $\lambda = 0.71073$ ) on a Bruker AXS Smart 1000 single-crystal diffractometer, equipped with a CCD area detector at 293(2) K. The struc-



ture was solved by direct methods using SIR97<sup>[22]</sup> and refined by full-matrix least-squares methods using the SHELXL-97 program.<sup>[23]</sup> The data reduction was performed using SAINT<sup>[24]</sup> and SADABS.<sup>[25]</sup> All the non-hydrogen atoms were refined with anisotropic atomic displacements, with the exclusion of the carbon atoms C21A and C22A at one lower rim, two *tert*-butyl groups, and two terminal carbon atoms at the lower rim chains, which were disordered over two different orientations with occupancy factors of 0.5 and refined with isotropic atomic displacements. The hydrogen atoms were included in the refinement at idealized geometries and refined "riding" on the corresponding parent atoms with common isotropic atomic displacements, which were refined, and with isotropic temperature factors 1.5-fold of their parent atoms. Geometric calculations and molecular graphics were performed with the PARST97 program.<sup>[26]</sup> Crystallographic data and experimental details for **2** and pseudorotaxane [**11**⊃DOV](T<sub>2</sub>O)<sub>2</sub> are reported in the Supporting Information.

### Acknowledgements

This research was partly supported by MIUR (Sistemi supramolecolari per la costruzione di macchine molecolari, conversione dell'energia, sensing e catalisi) and Regione Emilia-Romagna (Nanofaber NetLab). The authors thank the Centro Interdipartimentale di Misure "G. Casnati" for NMR measurements.

- [1] a) N. Sakai, J. Mareda, S. Matile, *Acc. Chem. Res.* **2005**, *38*, 79–87; b) T. Shimi, M. Masuda, H. Minamikawa, *Chem. Rev.* **2005**, *105*, 1401–1443; c) T. Sanji, N. Kato, K. Masako, M. Tanaka, *Angew. Chem.* **2005**, *117*, 7467–7470; *Angew. Chem. Int. Ed.* **2005**, *44*, 7301–7304.
- [2] See for example: a) I. Tabushi, Y. Kuroda, K. Yokata, *Tetrahedron Lett.* **1982**, *23*, 4601–4604; b) J. D. Hartgerink, J. R. Granja, R. A. Milligan, M. R. Ghadiri, *J. Am. Chem. Soc.* **1996**, *118*, 43–50; c) G. W. Orr, L. J. Barbour, J. L. Atwood, *Science* **1999**, *285*, 1049–1052; d) W. M. Leevy, J. E. Huettner, R. Pajewski, P. H. Schlesinger, G. W. Gokel, *J. Am. Chem. Soc.* **2004**, *126*, 15747–15753; e) J. H. van Maarseveen, W. S. Horne, M. R. Ghadiri, *Org. Lett.* **2005**, *7*, 4503–4506; f) M. E. Weber, W. Wang, S. E. Steinhardt, M. R. Gokel, W. M. Leevy, G. W. Gokel, *New J. Chem.* **2006**, *30*, 177–184.
- [3] a) *Calixarenes in the Nanoworld* (Eds.: J. Vicens, J. Harrowfield), Springer, Dordrecht, **2007**; b) K. S. J. Iqbal, P. J. Cragg, *Dalton Trans.* **2007**, 26–32; c) V. G. Organo, V. Sgarlata, F. Firouzbakht, D. M. Rudkevich, *Chem. Eur. J.* **2007**, *13*, 4014–4023; d) B. H. Hong, S. C. Bae, C.-W. Lee, S. Jeong, K. S. Kim, *Science* **2001**, *294*, 348–351; e) J. L. Atwood, L. J. Barbour, M. J. Hardie, C. L. Raston, *Coord. Chem. Rev.* **2001**, *222*, 3–32.
- [4] a) A. Arduini, F. Calzavacca, A. Pochini, A. Secchi, *Chem. Eur. J.* **2003**, *9*, 793–799; b) A. Arduini, F. Ciesa, M. Fragassi, A. Pochini, A. Secchi, *Angew. Chem.* **2005**, *117*, 282–285; *Angew. Chem. Int. Ed.* **2005**, *44*, 278–281.
- [5] F. Ugozzoli, C. Massera, A. Arduini, A. Pochini, A. Secchi, *Cryst-EngComm* **2004**, *6*, 227–232; A. Pochini, A. Secchi, *CrystEngComm* **2004**, *6*, 227–232.
- [6] A. Credi, S. Dumas, S. Silvi, M. Venturi, A. Arduini, A. Pochini, A. Secchi, *J. Org. Chem.* **2004**, *69*, 5881–5887.
- [7] a) V. Balzani, M. Venturi, A. Credi, *Molecular Devices and Machines—A Journey into the Nanoworld*, Wiley-VCH, Weinheim, **2003**; b) H. Tian, Q. C. Wang, *Chem. Soc. Rev.* **2006**, *35*, 361–374; c) V. Balzani, A. Credi, S. Silvi, M. Venturi, *Chem. Soc. Rev.* **2006**, *35*, 1135–1149; d) E. R. Kay, D. A. Leigh, F. Zerbetto, *Angew. Chem.* **2007**, *119*, 72–196; *Angew. Chem. Int. Ed.* **2006**, *45*, 72–191; e) S. Saha, J. F. Stoddart, *Chem. Soc. Rev.* **2007**, *36*, 77–92; f) B. Champin, P. Mobian, J. P. Sauvage, *Chem. Soc. Rev.* **2007**, *36*, 358–366.
- [8] K.-S. Jeong, K.-M. Hahn, Y. L. Cho, *Tetrahedron Lett.* **1998**, *39*, 3779–3782.
- [9] K. Kavallieratos, A. Danby, G. J. Van Berkel, M. A. Kelly, R. A. Schleben, B. A. Moyer, K. Bowman-James, *Anal. Chem.* **2000**, *72*, 5258–5264.
- [10] a) A. Arduini, E. Brindani, G. Giorgi, A. Pochini, A. Secchi, *J. Org. Chem.* **2002**, *67*, 6188–6194; b) A. Arduini, G. Giorgi, A. Pochini, A. Secchi, F. Ugozzoli, *J. Org. Chem.* **2001**, *66*, 8302–8308.
- [11] S. Le Gac, X. Zeng, O. Reinaud, I. Jabin, *J. Org. Chem.* **2005**, *70*, 1204–1210.
- [12] a) A. Arduini, L. Domiano, L. Ogliosi, A. Pochini, A. Secchi, R. Ungaro, *J. Org. Chem.* **1997**, *62*, 7866–7868; b) A. Arduini, R. Ferdani, A. Pochini, A. Secchi, *Tetrahedron* **2000**, *56*, 8573–8577.
- [13] A. Arduini, R. Ferdani, A. Pochini, A. Secchi, F. Ugozzoli, *Angew. Chem.* **2000**, *112*, 3595–3598; *Angew. Chem. Int. Ed.* **2000**, *39*, 3453–3456.
- [14] P. M. S. Monk, *The Viologens: Physicochemical Properties, Synthesis and Applications of the Salts of 4,4'-Bipyridine*, Wiley, New York, **1998**.
- [15] R. Ballardini, A. Credi, M. T. Gandolfi, C. Giansante, G. Marconi, S. Silvi, M. Venturi, *Inorg. Chim. Acta* **2007**, *360*, 1072–1082.
- [16] C. K. Mann, K. K. Barnes, *Electrochemical Reactions in Nonaqueous Systems*, Dekker, New York, **1970**.
- [17] The addition of the supporting electrolyte did not affect the stability of the [**11**⊃DOV]<sup>2+</sup> complex under our conditions.
- [18] According to molecular models, an efficient encapsulation of the viologen unit is afforded in pseudorotaxanes and rotaxanes containing the wheel **1** as a result of the presence of extended diphenylureido moieties.
- [19] S. Tsuzuki, K. Honda, T. Uchimar, M. Mikami, K. Tanabe, *J. Am. Chem. Soc.* **2000**, *122*, 3746–3753.
- [20] J. J. González, R. Ferdani, E. Albertini, J. M. Blasco, A. Arduini, A. Pochini, P. Prados, J. de Mendoza, *Chem. Eur. J.* **2000**, *6*, 73–80.
- [21] R. A. Binstead, SPECIFIT, Spectrum Software Associates, Chapel Hill, NC, **1996**.
- [22] A. Altomare, M. C. Burla, M. Camalli, G. L. Cascarano, C. Giacovazzo, A. Guagliardi, A. G. G. Moliterni, G. Polidori, R. Spagna, *J. Appl. Crystallogr.* **1999**, *32*, 115–119.
- [23] G. M. Sheldrick, SHELXL97, Program for Crystal Structure Refinement, University of Göttingen, Göttingen (Germany), **1997**.
- [24] SAINT, Software Users Guide, 6.0, Bruker Analytical X-ray Systems, **1999**.
- [25] G. M. Sheldrick, SADABS, Area-Detector Absorption Correction, 2.03, University of Göttingen, Göttingen (Germany), **1999**.
- [26] M. Nardelli, *J. Appl. Crystallogr.* **1996**, *29*, 296–296.

Received: May 16, 2007

Revised: August 8, 2007

Published online: September 26, 2007